

# Isotope fingerprints in elephant bone and ivory

J. C. Vogel, B. Eglinton & J. M. Auret

EMATEK Division, CSIR, Box 395, Pretoria, South Africa

THE isotopic composition of carbon and nitrogen as well as of strontium in animal bone is related to the environment in which the animal lived<sup>1-6</sup>. It can be assumed that this is also the case for lead isotopes. In theory, therefore, we have a way of pinpointing the origin of elephant ivory, which may be of value in conservation. Here we report that by analysing the isotope ratios of these elements, a clear distinction between several different populations of the African elephant can be made.

We used the isotope signatures to characterize elephant populations in different habitats in southern Africa (Fig. 1). In most cases bone from the jaws or ribs was used, but some samples of ivory were also included. The specimens came from the Knysna Forest on the south coast of the Cape Province, the Addo Elephant National Park in the southwest Cape, different areas of the Kruger National Park, East Transvaal, and the northern Namib Desert in Namibia. Three single samples from areas to the east of the latter group, namely East Kaokoveld, the Etosha Game Reserve and Caprivi, complete the list.

The factors expected to determine the isotope ratios of the various elements in the skeletons of elephants are briefly discussed below. In most parts of Africa the <sup>13</sup>C/<sup>12</sup>C ratio in animal tissue is determined primarily by the amount of (C<sub>4</sub>) grass ingested by the animal<sup>1</sup> and, thus, in the case of mixed feeders such as elephants, which both graze and browse, is to a degree dependent on the environment<sup>2</sup>. The <sup>15</sup>N/<sup>14</sup>N ratio in bone collagen of ungulates, is, again, higher in more arid habitats<sup>3,4</sup>. This may be ascribed, at least in part, to the higher <sup>15</sup>N levels of the local vegetation<sup>5</sup>, and for the rest it has been proposed to be the effect of drought stress on the protein metabolism of the animals themselves<sup>6</sup>. The carbon and nitrogen isotopes, even when taken together, do not, however, completely characterize the various elephant populations of southern Africa<sup>7</sup>. Only by adding a further independent isotope signature can this be achieved.

The <sup>87</sup>Sr/<sup>86</sup>Sr ratio in animal bone is determined by that of the strontium in the animal's plant diet, which is determined by the ratios in the soil and water of the area<sup>8,9</sup>. In most cases these ratios reflect those of the underlying rocks. <sup>87</sup>Sr is produced by the slow radioactive decay of <sup>87</sup>Rb, so that its abundance depends on the rubidium content and the age of the rock suites in the substrata of the area. Consequently, the higher the Rb/Sr ratio and the older the rock, the higher the <sup>87</sup>Sr/<sup>86</sup>Sr ratio will be.

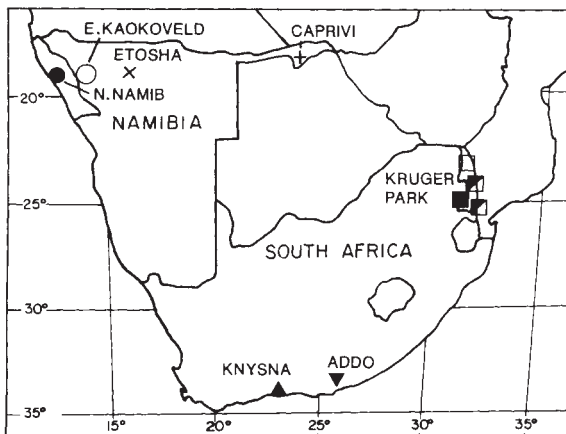


FIG. 1 Map of southern Africa indicating the localities from which samples of elephant bone were analysed. The same symbols are used in Fig. 2.

The lead isotopes, which are decay products of uranium and thorium, have not been used previously on bone material in the same way as have the strontium isotopes. Lead substitutes for calcium in a similar manner to strontium and the lead isotope ratios should thus also be characteristic of the underlying rocks.

Standard procedures were used to prepare samples for isotope analysis in suitable mass spectrometers. The results are listed in Table 1. <sup>13</sup>C analysis only distinguishes the Knysna specimens from the rest, whereas <sup>15</sup>N clearly distinguishes Knysna, Kruger Park and Addo samples, with the Namibian specimens falling between and overlapping the latter two groups. The <sup>87</sup>Sr, again, distinguishes the Namibian samples from the rest, the higher <sup>87</sup>Sr values being associated with areas on older, more felsic substrata (see Table 1). It is also noteworthy that the specimens from the Archaean granitic area in the far southwest of the Kruger Park have distinctly higher <sup>87</sup>Sr values than do those from the younger Mesozoic basalts in the far northeast, as is to be expected. The three lead isotopes show close correlation with each other, but do not effectively distinguish the different regions from each other, although there is a tendency for the isotope ratios in Addo and most of the Kruger Park specimens to be lower than those in Knysna and the Namib.

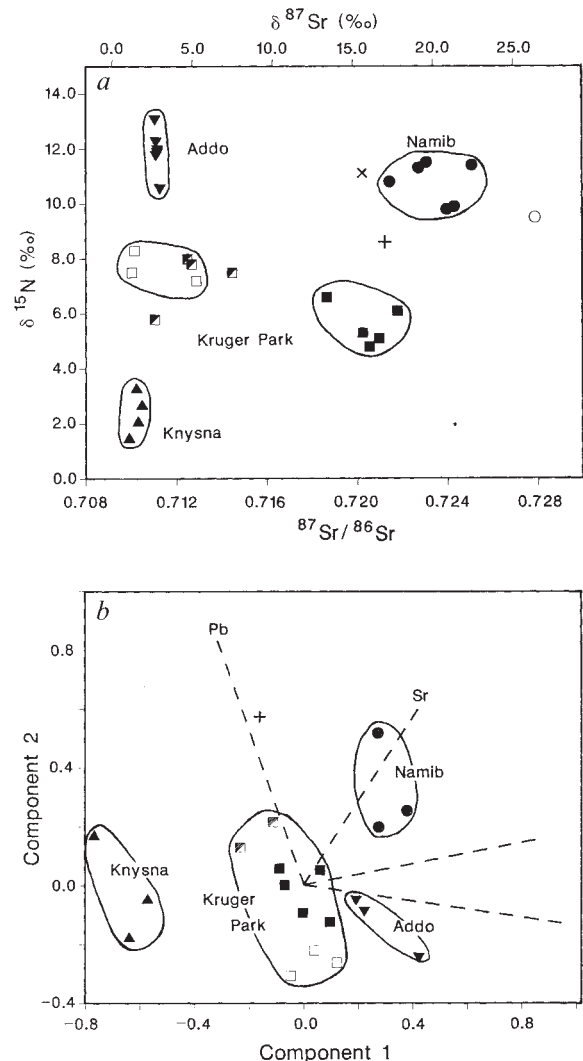


FIG. 2 a, Plot of the relative <sup>15</sup>N and <sup>87</sup>Sr contents of elephant bone, showing the complete separation of the different elephant populations from Knysna, Addo, Kruger Park and the N. Namib Desert (Table 1). The specimens belonging to specific populations are encircled. b, Plot of the first two principal components of the multivariate statistical analysis of the specimens for which measurements of the isotopic composition of carbon, nitrogen, strontium and lead were made.

TABLE 1 Isotope ratio measurements of elephant bone and tusk from localities in southern Africa\*

Sample no.	Locality	Main rock substrate	Material	$\delta^{13}\text{C}$ (%)	$\delta^{15}\text{N}$ (%)	$^{87}\text{Sr}/^{86}\text{Sr}$	$\delta^{87}\text{Sr}$ (‰)	$^{206}\text{Pb}/^{204}\text{Pb}$	$^{207}\text{Pb}/^{204}\text{Pb}$	$^{208}\text{Pb}/^{204}\text{Pb}$
B730	Knysna Forest, S Cape Prov	Palaeozoic sandstones, Table Mountain Group	Bone	-23.6	+3.0	0.710609	+2.0	17.295	15.561	37.435
B765			Bone	-23.8	+1.2	0.710281	+1.5	16.919	15.509	36.851
C4099	Kruger Park, E. Tvl*	Mesozoic marine seds, Uitenhage Group	Tusk	-24.5	+2.4	0.710845	+2.3			
C4100			Bone	-24.7	+1.8	0.710676	+2.1	18.039	15.724	38.905
			Average	-24.2	+2.1	0.710603	+2.0	17.417	15.598	37.730
			s.d.	$\pm 0.5$	$\pm 0.8$	$\pm 0.000236$	$\pm 0.3$	$\pm 0.569$	$\pm 0.112$	$\pm 1.058$
B733	Addo Elephant Park, SE Cape Prov.	Mesozoic marine seds, Uitenhage Group	Bone	-19.2	+12.0	0.711482	+3.2			
B734			Bone	-18.8	+11.7	0.711562	+3.3			
B735			Bone	-17.7	+10.3	0.711656	+3.5	17.078	15.502	36.859
B738			Bone	-17.1	+12.8	0.711442	+3.2	16.476	15.458	36.259
B739			Bone	-18.8	+11.6	0.711546	+3.3	17.118	15.538	37.165
B741			Bone	-17.5	+11.5	0.711484	+3.2			
	Average	-18.2	+11.7	0.711529	+3.3	16.891	15.499	36.761		
	s.d.	$\pm 0.9$	$\pm 0.8$	$\pm 0.000077$	$\pm 0.1$	$\pm 0.360$	$\pm 0.040$	$\pm 0.461$		
B770.1	Far SW. (Skukuza to Malelane)	Archaean granitoid gneisses	Bone	-18.9	+6.3	0.719014	+13.8	16.430	15.440	36.131
B770.3			Bone	-19.2	+5.8	0.720617	+16.1	16.804	15.698	36.821
B770.4			Bone	-20.1	+4.5	0.720915	+16.5	16.932	15.649	36.904
B770.5			Bone	-19.8	+4.8	0.721340	+17.1	16.363	15.419	36.037
B770.0			Bone	-20.3	+5.0	0.722530	+18.8	16.725	15.448	36.482
			Average	-19.7	+5.3	0.720883	+16.5	16.651	15.531	36.475
	s.d.	$\pm 0.6$	$\pm 0.7$	$\pm 0.001273$	$\pm 1.8$	$\pm 0.244$	$\pm 0.132$	$\pm 0.392$		
B773.1	Far NE (S of Pafuri)	Mesozoic basalts, Karoo Seq.	Bone	-20.0	+7.2	0.710417	+1.7	16.396	15.460	36.130
B773.2			Bone	-18.0	+8.0	0.710528	+1.9	16.612	15.463	36.336
B773.4			Bone	-19.0	+6.9	0.713263	+5.7	16.526	15.478	36.259
			Average	-19.0	+7.4	0.711403	+3.1	16.511	15.467	36.242
			s.d.	$\pm 1.0$	$\pm 0.7$	$\pm 0.001612$	$\pm 2.3$	$\pm 0.109$	$\pm 0.010$	$\pm 0.104$
C4069	Far SE (Crocodile Bridge)	Transitional	Tusk	-18.6	+7.2	0.714848	+8.0			
C4068			Bone	-20.0	+5.5	0.711428	+3.1	17.924	15.647	38.552
C4050	Mid S (Tshokwane)	Transitional	Tusk	-17.2	+7.7	0.712864	+5.2			
C4051			Bone	-19.7	+7.5	0.713054	+5.4	18.040	15.728	38.911
Namibia										
B846	N. Namib Desert	Mid-Late Proterozoic gneisses and schists	Bone	-18.6	+9.5	0.724338	+21.3	17.042	15.529	37.139
B847			Bone	-18.7	+11.1	0.725462	+22.9	18.012	15.718	38.869
B848			Bone	-17.8	+11.2	0.723448	+20.1	17.280	15.548	37.215
B849			Bone	-18.0	+9.6	0.724681	+21.8			
B851			Bone	-18.7	+10.5	0.721813	+17.8			
B853			Bone	-17.9	+11.0	0.723087	+19.6			
	Average	-18.3	+10.5	0.723805	+20.6	17.445	15.598	37.741		
	s.d.	$\pm 0.4$	$\pm 0.8$	$\pm 0.001297$	$\pm 1.8$	$\pm 0.506$	$\pm 0.104$	$\pm 0.978$		
B857	E Kaokoveld	Mid Proterozoic granitoid gneisses	Bone	-16.4	+9.2	0.728249	+26.9			
B316	Etosha Game Reserve	Cenozoic sands, Kalahari Group over	Bone	-17.9	+10.8	0.720615	+16.1			
B112	Caprivi	Late Proterozoic meta-seds	Bone	-21.7	+8.2	0.721590	+17.5	18.485	15.655	38.298

\*  $\delta^{13}\text{C}$ , Carbon isotope ratios expressed relative to the PDB reference standard;  $\delta^{15}\text{N}$ , nitrogen isotope ratios relative to atmospheric nitrogen;  $\delta^{87}\text{Sr}$ , strontium isotope ratios relative to average modern-day sea water (0.70920). The reproducibility of the measurements (1 s.d.) is better than 0.4% for carbon and nitrogen, 0.1% for strontium, and 0.1%, 0.1% and 0.2% for the three lead isotope ratios, respectively. Replicates of NBS SRM 987 strontium carbonate gave an isotope ratio of  $0.710275 \pm 16$  (1 s.d.,  $n=10$ ). Mass fractionation corrections for the lead ratios are based on replicates of NBS SRM 981.

† The four groups represent four different populations in the Park. The specimens from the Far SW are from at least three different herds; those from the Far NE are from two separate herds.

For the various elephant populations considered here, complete distinction, without any overlap, is achieved by plotting  $^{15}\text{N}$  against  $^{87}\text{Sr}$  (Fig. 2a).

As further populations from other parts of Africa are added, the characterization based on these two isotopes alone is bound to become less distinct, and multivariate analysis, using all the available isotopes, would be more appropriate. To illustrate this approach, isotope data for the 20 specimens for which lead isotope measurements are also available (using the  $^{206}\text{Pb}/^{204}\text{Pb}$  ratio as representative of the three lead isotopes) have been analysed using multivariate statistics, in the form of combined R- and Q-mode components analysis<sup>10</sup>, based on a correlation similarity matrix. Ninety-eight per cent of the total variance in the data set is explained by three components which are essentially dominated by the isotope ratios of C and N (component 1), Pb and Sr (component 2) and Sr (component 3). Distinction of the four populations is quite clear on a plot of component 1 against component 2 (Fig. 2b), although plots of the other components could be more effective in distinguishing separate localities within a region.

Most of our analyses were of bone, but there is no reason why ivory cannot also be used. The only difference would be

that a sample of ivory taken from the base of the tusk reflects the food intake during the last year or so of the life of the animal, whereas the bone is integrated over most of its lifetime. To check the validity of using ivory, three pairs of bone and ivory from the same animal were analysed (see Table 1). In all three cases the ivory values fall into the same grouping in Fig. 2a as do those of the bone. It can, therefore, be concluded with confidence that the combined analysis of  $^{15}\text{N}$  and  $^{87}\text{Sr}$  in tusks can provide a useful tool for establishing their origin. More distinctive fingerprinting can be achieved by adding other isotope signatures, notably those of lead, carbon and, possibly, sulphur. There would have to be a more complete survey of elephant habitats in the rest of Africa before the technique can be applied on a wide scale. In principle, however these isotope fingerprints in ivory can make a positive contribution towards monitoring the products of the endangered African elephant. □

Received 21 March; accepted 11 June 1990.

- Vogel, J. C. S. *Afr. J. Sci.* **74**, 298-301 (1978).
- Van der Merwe, N. J., Lee Thorp, J. A. & Bell, R. H. V. *Afr. J. Ecol.* **26**, 163-172 (1988).
- Heaton, T. H. E., Vogel, J. C., von la Chevallerie, G. & Collett, G. *Nature* **322**, 822-823 (1986).

4. Sealy, J. C., Van der Merwe, N. J., Lee Thorp, J. A. & Lanham, J. L. *Geochim. cosmochim. Acta* **51**, 2707-2717 (1987).
  5. Heaton, T. H. E. *Oecologia* **74**, 236-246 (1987).
  6. Ambrose, S. H. & DeNiro, M. J. *Oecologia* **69**, 395-406 (1987).
  7. Vogel, J. C., Talma, A. S., Hall-Martin, A. & Viljoen, P. J. S. *Afr. J. Sci.* **86**, 147-150 (1990).
  8. Ericson, J. E. *J. hum. Evol.* **14**, 503-514 (1985).
  9. Sealy, J. C., Van der Merwe, N. J., Sillen, A., Krueger, F. J. & Krueger, H. W. *J. archaeol. Sci.* (in the press).
10. Davis, J. C. *Statistics and Data Analysis in Geology* (Wiley, New York, 1986).

ACKNOWLEDGEMENTS. We thank Dr A. Hall-Martin, Skukuza, and P. J. Viljoen, Pretoria, for supplying most of the samples, G. von la Chevallerie, Y. Stander and G. Jakob for assistance with the laboratory preparations, and S. Talma and T. Heaton for supervising the carbon and nitrogen mass spectrometric analyses.

## Maintenance of B-cell memory by long-lived cells generated from proliferating precursors

Birgit Schitteck & Klaus Rajewsky

Institute for Genetics, University of Cologne, Weyertal 121, D-5000 Cologne 41, FRG

A BASIC feature of T-cell dependent antibody responses is the generation of memory: on a second contact with an antigen a secondary response is produced in which somatically mutated antibodies with increased affinity are synthesized<sup>1</sup>. Memory can persist for long periods of time. This has classically been ascribed to the generation of long-lived memory B cells<sup>2,3</sup>. However, it is also possible that persisting antigen, on which memory may depend<sup>4</sup>, maintains a population of cycling memory cells under continuous selection<sup>5</sup> or continuously recruits newly generated B cells into the memory B-cell compartment<sup>6</sup>. To discriminate between these mechanisms we have now directly analysed the proliferative activity in the memory B-cell compartment of the mouse by measuring bromodeoxyuridine incorporation *in vivo*. We show that after an initial phase of extensive proliferation after primary immunization, memory cells can persist in the organism for extended periods of time in the absence of cell division.

In accordance with the work of Hayakawa *et al.*<sup>7</sup>, we raised specific memory B cells in mice by immunization with the highly fluorescent protein phycoerythrin (PE) and characterized them as PE-binding cells that express the B-cell marker B220 and low levels of surface immunoglobulin differing in class from IgM and IgD as expressed by naive B cells. Using magnetic cell sorting and flow cytometry in combination, we analysed these cells directly for their proliferative activity *in vivo*. The outline of the experiment is given in Fig. 1. At various times after immunization, bromodeoxyuridine (BrdU; 1 mg ml<sup>-1</sup>) was added to the drinking water of the animals, for various periods of time. Dividing lymphoid cells incorporate BrdU into their DNA under these conditions, and the proliferative behaviour of BrdU-labelled B lineage cells is not different from that of unlabelled cells<sup>8,9</sup>. At the time of analysis, spleen cells were isolated, enriched for IgM<sup>-</sup>IgD<sup>-</sup> B cells on a magnetic cell sorter (MACS)<sup>10</sup>, and stained with PE and an anti-B220 antibody. The cells could then be processed in either of two ways: flow cytometric analysis and cell sorting allowed quantitation and functional and morphological analysis of PE binding memory cells; alternatively, the cells were fixed, stained with an anti-BrdU antibody and analysed for BrdU incorporation by three-colour flow cytometry.

PE-binding, B220-positive (B220<sup>+</sup>PE<sup>+</sup>) cells were readily detectable among the IgM<sup>-</sup>IgD<sup>-</sup> spleen cells of PE-immunized mice (see Fig. 2a). When these cells were examined under the fluorescence microscope, they turned out to be small lymphocytes, negative for IgM and IgG1 in the cytoplasm. To confirm that these cells are functionally active memory cells, we tested them for their ability to produce a secondary antibody response *in vitro*, as described earlier<sup>7</sup>. For this purpose, PE-

binding (B220<sup>+</sup>PE<sup>+</sup>) and nonbinding B cells (B220<sup>+</sup>PE<sup>-</sup>) isolated from the spleens of mice immunized with PE 7 or 12 weeks earlier were cultured in the presence or absence of helper T cells (CD4<sup>+</sup>) from PE-immunized mice (Table 1). After 14 days the culture fluids were analysed for the presence of PE-specific IgG1 antibodies. As few as 250 B220<sup>+</sup>PE<sup>+</sup> cells, but not B220<sup>+</sup>PE<sup>-</sup> cells produce a strong IgG1 anti-PE-response when (and only when) cultured together with PE-specific helper T cells (Table 1). This confirms that in the PE-primed animals PE-specific memory B cells are located in the B220<sup>+</sup>PE<sup>+</sup> population and that the antibody response measured is not due to plasma cell contamination.

To determine the proliferative activity of these memory cells, the cells were analysed for BrdU incorporation *in vivo*. Feeding of BrdU to the mice was started either 1 day, 4 weeks, 10 weeks or 20 weeks after priming, and stopped 1, 3, 5 or 7 weeks later; the spleen cells of the animals were processed as shown in Fig. 1. Representative staining patterns are shown in Fig. 2. Plotted is either PE against anti-B220 (Fig. 2a) or PE against anti-BrdU-staining (Fig. 2b). To determine the ratio of labelled versus unlabelled cells among the memory cells, we gated on B220<sup>+</sup>PE<sup>+</sup> cells (Fig. 2a), collected 1,000-5,000 cells in this fraction, analysed the BrdU-staining profile (Fig. 2c-f) and calculated the percentage of BrdU-labelled cells in this population.

Almost all of the B220<sup>+</sup>PE<sup>+</sup> cells (92%) divide within the first five weeks after priming (Fig. 3a). That the values do not reach 100% could indicate that this population contains cells that do not divide at all. More likely, this represents a problem in the evaluation of the staining data, as negative and positive populations were not always fully separated. When BrdU-treatment is

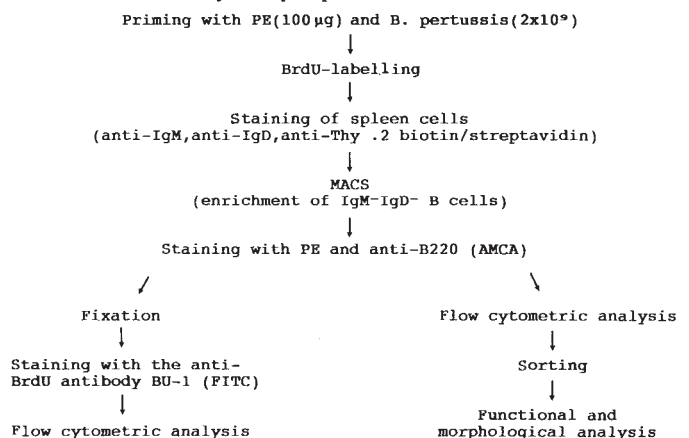


FIG. 1 Schematic outline of the experiment.

METHODS. BALB/c mice or BALB/c mice congenic for the IgH<sup>b</sup> haplotype (CB.20) were immunized by intraperitoneal injection of 100 µg PE (gift of Dr W. Müller) and 2 × 10<sup>9</sup> *Bordetella pertussis* organisms as an adjuvant. No difference in the response of the two strains was observed. BrdU-labelling was done by feeding the mice for various time periods after priming with 1 mg BrdU (Sigma) per ml drinking water<sup>8,9</sup>. Spleen cells of three mice from a given experimental group were pooled and erythrocytes lysed in 0.8% NH<sub>4</sub>Cl. To enrich for IgM<sup>-</sup>IgD<sup>-</sup> B cells we used the method of magnetic cell sorting as described previously<sup>10</sup>. Briefly, spleen cells were stained with the biotinylated antibodies RS3.1 (ref. 19) or MBB6 (ref. 20) (anti-IgM), 10.4.22 (ref. 21) or 4/4D7 (a gift from Dr T. Tokuhisa) (anti-IgD) and H013-14 (anti-Thy-1.2)<sup>22</sup>. The cells were then incubated with streptavidin (Boehringer) and, in a third step, with superparamagnetic biotinylated microparticles. Eight to eighteen percent of the spleen cell population remained unlabelled by this procedure and were enriched to 85-95% using a MACS<sup>10</sup>. The recovery was 70-80%. The enriched cells were stained with PE (10 µg per 5 × 10<sup>7</sup> cells) and with the anti-B220 antibody RA3.6B2 (ref. 23) coupled to AMCA (Amino-methyl-coumarin-acetic acid)<sup>24</sup> (10 µg per 5 × 10<sup>7</sup> cells). Cells were fixed in 70% ethanol, washed in PBS and stained with the anti-BrdU antibody BU-1 (refs 25, 26) (culture supernatant; 30 µg per 2 × 10<sup>7</sup> cells) (kindly provided by Dr N. Gonchoroff) and with an anti-IgG2a<sup>a</sup> antibody (Ig(1a)B.3)<sup>21</sup> coupled to fluorescein-isothiocyanate (FITC; 10 µg per 5 × 10<sup>7</sup> cells). Using this anti-BrdU antibody it is not necessary to denature the cellular DNA by acid or base treatment, which would destroy PE-staining of the cells.